LANGMUIR

Article

pubs.acs.org/Langmuir

Electrocatalytic Reduction of Oxygen on Platinum Nanoparticles in the Presence and Absence of Interactions with the Electrode Surface

Nevena Ostojic and Richard M. Crooks*

Department of Chemistry and the Center for Nano- and Molecular Science and Technology, The University of Texas at Austin, 105 East 24th Street, Stop A5300, Austin, Texas 78712-1224, United States

Supporting Information

ABSTRACT: We report that ultraviolet/ozone (UV/O_3) treatment can be used to remove sixth-generation, hydroxyl-terminated poly(amidoamine) (PAMAM) dendrimers from dendrimer-encapsulated Pt nanoparticles (Pt DENs) previously immobilized onto a pyrolyzed photoresist film (PPF) electrode. Results from X-ray photoelectron spectroscopy, scanning transmission electron microscopy, and electrochemical experiments indicate that removal of the dendrimer proceeds without changes to the size, shape, or electrocatalytic properties of the encapsulated nanoparticles. The UV/O_3 treatment did not damage the PPF electrode. The electrocatalytic properties of the DENs before and after removal of the dendrimer were nearly identical.

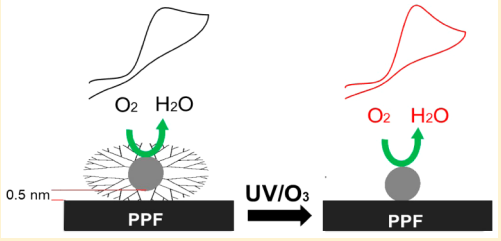

INTRODUCTION

In this paper, we report a method for cleanly removing dendrimers from surface-confined dendrimer-encapsulated Pt nanoparticles (Pt DENs),[1−9] without measurably changing their size or shape (Scheme 1). The results of this study are important for two reasons. First, they lead to a general means for preparing highly monodisperse, stabilizer-free mono- and bimetallic nanoparticles (NP) in the 0.5−3.0 nm size range. Second, and more specifically, we are now in a position to begin answering fundamental questions about how the presence of a dendrimer affects the catalytic properties of DENs.[10] Accordingly, we begin this set of studies by discussing how the dendrimer affects the oxygen reduction reaction (ORR) electrocatalyzed by Pt NPs in the presence and absence of dendrimers.

Scheme 1

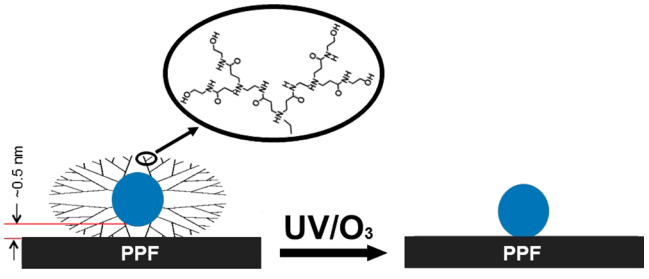

First synthesized by Vogtle and co-workers in 1978,[11] dendrimers are branched, spherical macromolecules widely used to encapsulate objects ranging from NPs to drugs.[12−16] Poly(amidoamine) (PAMAM) dendrimers are a dendrimer subclass that consists of an alkyl-diamine core, amidoamine branches, and a vast range of peripheral functionalities (Scheme 1).[16] The size of PAMAM dendrimers depends on the number of reaction cycles carried out during the synthesis.[16] For example, seven iterations of Michael addition followed by amidation yields a sixth-generation (G6) dendrimer having a calculated diameter of ∼6.7 nm.[17,18] DENs are usually prepared in PAMAM dendrimers in two steps. First, the dendrimers are mixed with metal ions, which partition into the dendrimer interior. The stoichiometric ratio between the dendrimer and the metal ions determines the final size of the encapsulated NP. Second, a strong reducing agent, such as BH_4^-, is added to the solution. This results in reduction of the ions and subsequent intradendrimer agglomeration of the resulting metal atoms.[1,19]

DENs usually have diameters between ∼0.5−2.2 nm,[3] but they can be smaller[20,21] or larger. In addition to acting as templates, dendrimers are also stabilizers that prevent aggregation of DENs in solution. Unlike most stabilizers, however, dendrimers do not passivate the surface of their encapsulated NPs. This means that DENs are good models for studying homogeneous and heterogeneous catalytic reactions in a broad range of solvents.[22−24] However, in the absence of a good solvent, like water or methanol, or in the gas phase, dendrimers collapse around the NPs rendering them inactive.[3,25−30] Under these conditions, therefore, the presence of the dendrimer renders the templated NPs catalytically inactive. Another consequence of the presence of the dendrimer is that immobilized DENs are not in direct contact with the support material (Scheme 1a), for example, an electrode. For fundamental NP catalysis studies in which experimental results are compared to first-principles calculations, this is good because it removes the complexity of NP-

Received: July 12, 2016
Revised: August 24, 2016
Published: September 19, 2016

DOI: 10.1021/acs.langmuir.6b02578
Langmuir 2016, 32, 9727−9735

support interactions from the theoretical description of the system.[5,9,31−37] Now, however, we are ready to begin including this additional level of complexity into our research, and therefore it has become necessary to find a way to remove the dendrimers from the DENs so that the metal is in direct contact with the substrate (Scheme 1b).

As will be discussed in more detail later, we have found that UV/O_3 is effective for cleanly eliminating dendrimers from DENs. Before settling on UV/O_3, we also considered plasmas and heat treatments. Previous studies suggested, however, that these methods generally lead to irreversible changes in NP size, shape, and distribution.[6,38−40] By contrast, UV/O_3 has previously been used to decompose solution-phase dendrimers and other organic capping agents with and without encapsulated NPs.[38,41,42] For example, Rosal and co-workers recently reported that G3 amine-terminated PAMAM dendrimers are completely decomposed by O_3 within 1 min.[41] The authors explained that decomposition arises from oxidation of dendritic amines, which results in highly oxidized fragments. Similarly, Somorjai and co-workers studied the decomposition of G4 hydroxyl-terminated PAMAM dendrimers (G4-OH) with and without encapsulated Pt and Rh NPs. This study showed that after 6 h of the UV/O_3 exposure, ∼ 60% of the overall dendrimer structure was destroyed.[42] The same group also used the UV/O_3 technique for removal of poly(vinylpyrrolidone) and tetradecyl tributylammonium bromide capping agents from Pt NPs.[38] In this study, the TEM data indicated that after 2 h of the UV/O_3 treatment the Pt NPs retained their original size and shape.

As mentioned earlier, we are interested in studying how supports cooperate with metal nanoparticles to catalyze electrochemical reactions like the ORR. There have been a few key studies in this regard that predate our own interest. For example, it has been shown that direct interactions between metal NPs and metal-oxide or metal-phosphate supports enhance electrocatalytic activity for the ORR.[43−47] Specifically, Alonso-Vante and co-workers showed that Pt NPs supported on a titanium dioxide (TiO_2)-modified carbon support (C/TiO_2/Pt) exhibit higher electrocatalytic activity for the ORR compared to the same Pt NPs deposited directly onto a carbon support (C/Pt).[43] The XPS analysis of the two electrocatalysts revealed that the effect of TiO_2 on Pt NPs is the result of a superposition of charge transfer and lattice strain. Adzic and co-workers demonstrated that Pt supported on a NbO_2-modified C support (C/NbO_2/Pt) experiences suppressed oxidation compared to Pt supported on carbon support (C/Pt) due to lateral repulsion between PtOH and oxide species from NbO_2.[44] They showed that this in turn results in 3 times higher Pt mass activity for the ORR compared to the commercial C/Pt electrocalayst. The Adzic group has also studied metal NP/support interactions for electrooxidation of alcohols, and these reactions are also accelerated by the presence of appropriate supports.[48−52]

In the remainder of this report, we will show that UV/O_3 treatment can be used to remove G6-OH immobilized on pyrolyzed photoresist film (PPF) supports (electrodes) in the presence of DENs. Importantly, the original size and shape of Pt DENs are conserved after dendrimer removal. The UV/O_3 treatment oxidizes ∼10% of the surface of encapsulated Pt NPs, but it is possible to remove this oxide electrochemically. More interestingly, we find that the Pt DEN-modified PPF electrodes are slightly more active for the ORR in the absence of the dendrimer.

EXPERIMENTAL SECTION

Chemicals and Materials. All chemicals were used as received. These include 1-decanethiol (96%, Alfa Aesar) and NaOH (Fischer Scientific). The following were obtained from Sigma-Aldrich: CH_2Cl_2, $CuSO_4$, $NaBH_4$, H_2SO_4 (+98%, trace metal grade), and K_2PtCl_4. The purge gas for the UV/O_3 system was O_2 (99.9999%, Praxair, Austin, TX).

G6-OH dendrimers were purchased as a 10−25% methanol solution from Dendritech, Inc. (Midland, MI). Prior to use, the methanol was removed under vacuum. Deionized (DI) water having a resistivity of 18.2 MΩ-cm (Milli-Q gradient system, Millipore) was used for the preparation of all aqueous solutions.

Fabrication of PPF Electrodes. PPF electrodes[53−56] were fabricated following a procedure previously reported by our group.[25] Briefly, quartz slides were cleaned sequentially in acetone, ethanol, and DI water for 10 min each. The quartz slides were further rinsed under running DI water for 1 min and then heated at 200 °C for 15 min. Next, positive-tone photoresist (AZ 1518, Capitol Scientific, Inc., Austin, TX) was spin-coated onto the slides for 10 s at 500 rpm, 45 s at 3500 rpm, and for 5 s at 500 rpm. Finally, the slides were soft baked for 1 min at 100 °C and left to cool to room temperature (24 ± 1 °C). The spin coating and soft baking processes were repeated a second time.

The photoresist-coated quartz slides were patterned by exposure to UV light through a photomask. Next, AZ 400 K developer, diluted 25% (v/v) with DI water, was used to develop the exposed photoresist. Finally, the photoresist was pyrolyzed in a quartz tube furnace under a constant flow (100 sccm) of forming gas (5% H_2 plus 95% N_2). The furnace temperature was increased from 25 to 1000 °C at 5 °C/min, held at 1000 °C for 1 h, and then cooled to 25 °C. The resulting PPF slide was then diced into individual electrodes using a diamond-tipped pen. The individual PPF electrodes were then rinsed under a gentle flow of DI water and dried under flowing N_2.

Synthesis of DENs. Pt DENs were synthesized using a previously published procedure based upon galvanic exchange.[19,57] Specifically, 1.0 mL of a 100.0 μM aqueous G6-OH dendrimer solution was further diluted with 8.68 mL of DI water. Next, 55 equiv of 20.0 mM $CuSO_4$ were pipetted into the G6-OH solution. The solution was sealed and stirred under N_2 for 15 min. Next, a 5-fold molar excess of aqueous 1.0 M $NaBH_4$ solution was added dropwise under N_2 to reduce intradendrimer Cu^{2+} to Cu NPs. The reduction was carried out for 45 min, and then the pH of the resulting G6-OH(Cu_{55}) DEN solution was adjusted to 3.0 using 1.0 M $HClO_4$. Finally, sufficient aqueous 10.0 mM $PtCl_4^{2-}$ (Pt^{2+}:Cu = 1) was added dropwise (under N_2) to initiate galvanic exchange, and then the solution was sealed and left to stir for 60 min under N_2. After purification by dialysis, STEM was used to determine the size distribution of the Pt DENs. One final point: the notation used to denote the DENs in this study, for example G6-OH(Pt_{55}), is simply a representation of the Pt^{2+}:G6-OH ratio used to prepare these materials and is not meant to imply that every DEN contains exactly 55 atoms of Pt.

The Pt DENs were immobilized atop PPF electrodes by immersing the latter in the Pt DENs solution (pH 3.0) for 60 min. Next, the electrodes were rinsed under a gentle flow of DI water and dried under flowing N_2. The newly formed PPF/G6-OH(Pt_{55}) electrodes were left to dry for at least 90 min prior to use.

Electrochemical Characterization. Electrochemical measurements were obtained using a CH Instruments model CHI700D Electrochemical Analyzer (Austin, TX). The electrochemical cell was fabricated from Teflon and used a Viton O-ring to define the area of the working electrode (12.4 mm^2). For all electrochemical experiments, a $Hg/HgSO_4$ reference electrode (MSE, CH Instruments) and a Pt wire counter electrode were used. To avoid poisoning the working electrode with Hg, resulting from leakage of the reference electrode, the working and reference electrodes were separated by a glass frit. Cyclic voltammograms (CVs) were obtained using aqueous 0.5 M H_2SO_4 solutions.

UV/O_3 Treatment. Individual PPF/G6-OH(Pt_{55}) electrodes were placed in the middle of the UV/O_3 chamber (PSD-UV4 with

DOI: 10.1021/acs.langmuir.6b02578
Langmuir 2016, 32, 9727−9735

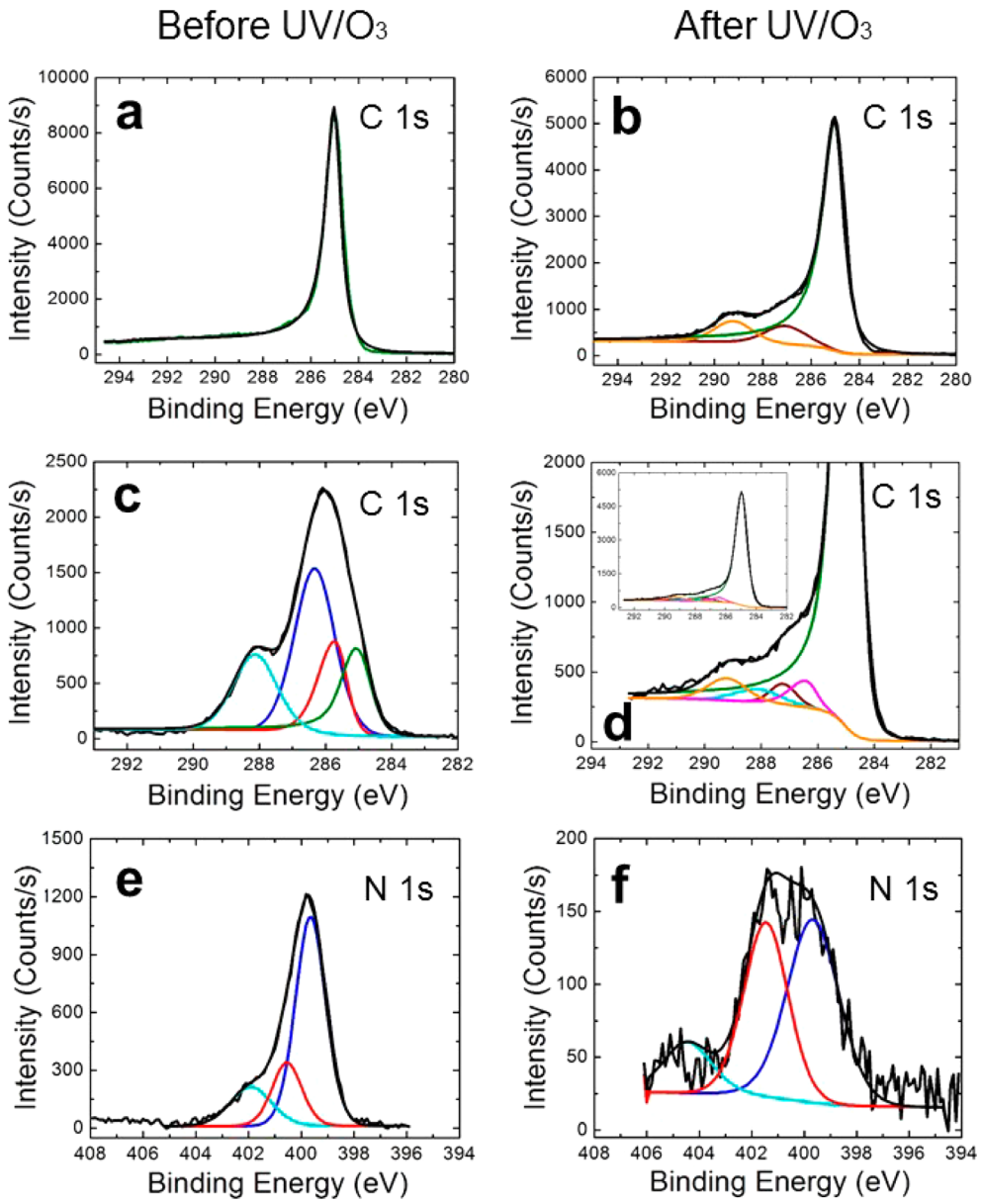

Figure 1. High-resolution XPS spectra in the C 1s region for a PPF electrode before (a) and after (b) UV/O_3 treatment. High-resolution XPS C 1s region of a PPF/G6-OH(Pt_{55}) electrode before (c) and after (d) UV/O_3 treatment. High-resolution XPS N 1s region of a PPF/G6-OH(Pt_{55}) electrode before (e) and after (f) UV/O_3 treatment.

OES1000D, Novascan Technologies, Ames, IA) and treated for 2.25 h using the following protocol, which we found to be critical for maximum dendrimer decomposition and minimal Pt NP surface oxidation.

First, the vacuum was turned on and an external supply of O_2 was introduced into the chamber at 259 mmHg for 10 min. Second, the O_2 flow was stopped and the UV lamp was turned on for 5 min. After turning off the UV lamp, the chamber was purged with O_2 for 3 min. This step was repeated two additional times. Third, the O_2 flow was stopped and the UV lamp was turned on for 15 min. The UV lamp was then turned off, and the chamber was purged with O_2 for 2 min. Fourth, the O_2 flow was stopped and the UV lamp was turned on for 30 min. After 30 min, the UV lamp was turned off and the chamber was purged with O_2 for 2 min. This step was repeated twice, and then the O_2 flow was stopped and the UV lamp was turned on for an additional 45 min. At this point the substrate was removed from the UV/O_3 chamber used within 30 min.

X-ray Photoelectron Spectroscopy (XPS). XPS samples were prepared by immobilizing Pt DENs atop PPF electrodes as previously described in the "Synthesis of DENs" section. XPS was carried out using a Kratos Axis Ultra spectrometer (Chestnut Ridge, NY) having an Al K_α source. Samples were grounded using metal holders. Careful placement of the PPF/G6-OH(Pt_{55}) electrode made it possible to characterize the same location before and after UV/O_3 treatment. This was necessary because the G6-OH(Pt_{55}) sample did not dry uniformly after dropping onto the PPF support.

XPS spectra were collected using a 0.10 eV step size and a band-pass energy of 20 eV. An electron flood gun was used to neutralize charge on the samples. Binding energies were calibrated against the C 1s line of PPF (285.0 eV).[58] CasaXPS (version 2.3.15, Casa Software, Teignmouth, UK) was used for peak fitting and analysis. A mixed Gaussian/Lorentzian model was used for symmetric line-shapes, while an asymmetric Lorentzian model was applied for asymmetric line shapes.

Scanning Transmission Electron Microscopy (STEM) and Scanning Electron Microscope (SEM). STEM images were obtained using a JEOL-2010F transmission electron microscope having a point-to-point resolution of 0.19 nm. Samples were prepared

DOI: 10.1021/acs.langmuir.6b02578
Langmuir 2016, 32, 9727−9735

by pipetting 2.0 μL of the G6-OH(Pt_{55}) solution onto a lacey-carbon-over-Ni TEM grid (Electron Microscopy Sciences, Hatfield, PA) and then drying in air on the grid overnight prior to analysis.

SEM images were collected using an EI Quanta 650 microscope with an accelerating voltage of 15 kV.

RESULTS AND DISCUSSION

Effect of UV/O_3 on PPF Substrates. The UV source used for the UV/O_3 treatment emits at 184.9 and 253.7 nm.[38] Oxygen absorbs at 184.9 nm to yield O_3. Subsequently, O_3 absorbs at 253.7 nm and decomposes to form atomic oxygen.[59] Atomic oxygen is a strong oxidant, which reacts with organics to yield volatile substances including CO_2, N_2, and H_2O.[38,59,60]

In the present study, we used XPS extensively to study the effect of UV/O_3 on dendrimer decomposition. Reliable conclusions, however, require careful control experiments so this investigation began with a study of the effects of UV/O_3 on naked PPF electrodes. The fabrication of the PPF electrodes and the protocol for UV/O_3 treatment are provided in the Experimental Section, but it amounts to a 2.25 h exposure.

Prior to UV/O_3 (Figure 1a), the C 1s region of the XPS spectrum of a naked PPF electrode consists of a single peak at 285.0 eV. This corresponds to the C−C bonds of the PPF substrate.[25,61] Following UV/O_3 exposure, however, the intensity of this peak decreases and two new oxidation products, corresponding to phenolic and carboxylic carbon,[25,58,61] are observed at 287.0 and 289.2 eV, respectively (Figure 1b). High-resolution analysis of the O 1s region confirms oxidation of the PPF surface, with the intensity of the surface oxygen peak increasing by a factor of 3 (Supporting Information, Figure S-1). No nitrogen was observed on the PPF surface before or after UV/O_3 exposure.

In addition to the XPS analysis, the effect of UV/O_3 treatment on the PPF electrodes was also examined by SEM (Figure S-2). Prior to UV/O_3 treatment, the surface of PPF electrodes is remarkably smooth and uniform.[25,61] Importantly, there are no discernible changes to the morphology of the PPF surface after exposure.

Effect of UV/O_3 on Pt DENs. We also used XPS to examine the effect of UV/O_3 on Pt DEN-modified PPF surfaces (PPF/G6-OH(Pt_{55})). Before exposure, the C 1s spectrum can be deconvoluted into four peaks (Figure 1c). The green-colored peak at the lowest binding energy (BE) (285.0 eV) arises from the underlying PPF support, indicating that the PPF electrode is not completely covered by the Pt DENs.[62] The red peak at 285.6 eV corresponds to aliphatic carbons of the dendrimer, and the blue peak at 286.3 eV is due to the C−OH, C−N(amine), and C−N(amide) functionalities of the dendrimer. The final peak (turquoise) at the highest BE (288.0 eV) can be fit to the carbonyl carbons of the dendrimer.[39]

After the UV/O_3 treatment, changes in all four carbon regions are observed. Specifically, the green peak at 285.0 eV, corresponding to the underlying PPF electrode, becomes dominant after the dendrimers are removed from the PPF surface. The red and blue peaks that were previously observed separately coalesce in a single peak (purple) at 286.4 eV. The dark red peak at 287.2 eV and the orange peak at 289.2 eV can be assigned to phenolic and carboxylic carbon, respectively. As discussed earlier, these peaks arise from the oxidation of the underlying PPF support. Finally, the turquoise carbonyl peak of the dendrimer is still observed at ∼288.0 eV, but at a much lower intensity than before UV/O_3 exposure. Comparison of the intensities of dendrimer C 1s peaks before and after UV/O_3 treatment, indicates that only ∼8% of the overall dendrimer C signal remains after UV/O_3 (Tables 1 and 2).

Table 1. Summary of XPS Peak Assignments, Positions, Areas, and Concentrations for a PPF/G6-OH(Pt_{55}) Electrode before UV/O_3 Treatment

element	assignment	position (eV)	area	percent concentration
C 1s	C−C bonds (PPF substrate)	285.0	1662.6	16.9
C 1s	aliphatic	285.6	1366.0	14
C 1s	hydroxyl, amine, and amide	286.3	3261.8	33
C 1s	carbonyl	288.0	1633.1	17
N 1s	amines	399.7	2180.1	12
N 1s	amides	400.6	646.8	3.6
N 1s	protonated amines	401.9	556.7	3.1
Pt 4f	metallic (Pt $4f_{7/2}$)	72.0	401.9	0.26
Pt 4f	metallic (Pt $4f_{5/2}$)	75.2	192.5	0.13

Table 2. Summary of XPS Peak Assignments, Positions, Areas, and Concentrations for a PPF/G6-OH(Pt_{55}) Electrode after UV/O_3 Treatment

element	assignement	position (eV)	area	percent concentration
C 1s	C−C (PPF substrate)	285.0	9304.5	84
C 1s	aliphatic, hydroxyl, amine, and amide	286.4	336.1	3.0
C 1s	phenolic	287.2	242.2	2.1
C 1s	carbonyl	288.0	264.3	2.3
C 1s	carboxylic	289.2	389.6	3.5
N 1s	amines	399.7	242.2	2.1
N 1s	amides	401.5	352.3	1.7
N 1s	protonated amines	404.3	112.1	0.50
Pt 4f	metallic (Pt $4f_{7/2}$)	72.2	839.4	0.48
Pt 4f	hydroxide	72.9	92.6	0.050
Pt 4f	metallic (Pt $4f_{5/2}$)	75.4	403.3	0.23
Pt 4f	hydroxide	76.2	50.6	0.030
Pt 4f	oxide	79.0	19.0	0.010

The N 1s spectrum of the PPF/G6-OH(Pt_{55}) electrode (Figure 1e) consists of three peaks. The highest one (blue) is at 399.7 eV and is assigned to amine nitrogens, while the red peak (400.6 eV) corresponds to amide nitrogens.[39] The final peak, observed at 401.9 eV (turquoise), arises from protonated amines.[19] Recall that the DEN-modified substrates were prepared at pH 3.0, so it is reasonable to find this species present. Nevertheless, the identity of this peak was confirmed by immobilizing G6-OH dendrimers at four different pH values (9.0, 7.5, 5.0, 3.0) on PPF electrodes, and then analyzing the resulting samples using XPS (Supporting Information, Figure S-3). The spectra reveal that at pH values of 9.0 and 7.5 only two nitrogen peaks are observed, corresponding to amine and amide groups. As the pH value is lowered to 5.0, however, a new peak slowly emerges at higher BE. It becomes pronounced at pH 3.0, and hence our assignment to protonated amines.[19] The experimentally determined amide:amine nitrogen ratio is 1:3.3, which is not consistent with the ratio of 2:1 calculated based on the dendrimer structure. This lower ratio has been observed before, however, and it may be a consequence of the amide signal being screened compared to the amine signal.[39]

After the UV/O_3 treatment, the same nitrogen regions are observed in the N 1s spectrum, but at much lower intensities

DOI: 10.1021/acs.langmuir.6b02578
Langmuir 2016, 32, 9727−9735

and with increased spacing between the peaks (Figure 1f). The relative intensities of the N 1s peaks before and after UV/O_3 treatment suggest that only ~23% of the original N signal is retained (Tables 1 and 2).

Effect of UV/O_3 on Pt DENs. Thus, far we have focused exclusively on the effect of UV/O_3 treatment on the dendrimer itself, but now we turn our attention to the encapsulated Pt DENs. Prior to UV/O_3 treatment, XPS indicates that two Pt 4f peaks are present at 72.0 eV (Pt $4f_{7/2}$) and 75.2 eV (Pt $4f_{5/2}$) (Figure 2a). Although, these BE values are higher than expected

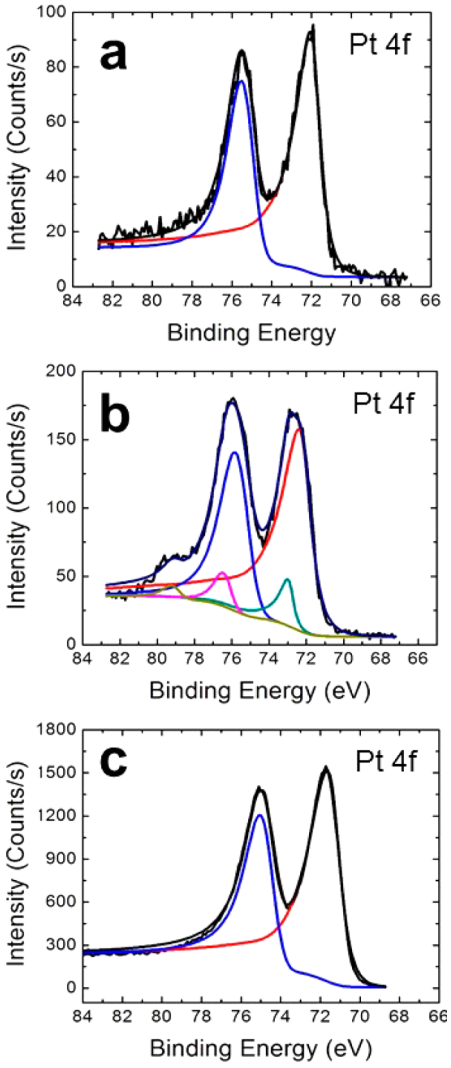

Figure 2. High-resolution XPS spectra in the Pt 4f region for a PPF/G6-OH(Pt_{55}) electrode (a) before and (b) after UV/O_3 treatment. (c) Same as panel b, but after 10 electrochemical scans (scan rate = 50 mV/s) in an Ar-purged, aqueous 0.5 M H_2SO_4 solution to reduce the surface oxide created during the UV/O_3 treatment.

for metallic Pt (71.2 for Pt $4f_{7/2}$),[26] we[25,57] and others[39] have previously observed this situation for DENs. The shift toward higher BE may result from the small size of the Pt NPs.[57]

Figure 2b presents the Pt XPS spectrum after UV/O_3 treatment. In this case, three new peaks emerge. The peaks at 72.9 and 76.2 eV are assigned to $Pt(OH)_2$, while the peak at 79.0 eV can be fit to PtO. These oxygenated species on the DEN surface are a consequence of the oxidizing power of atomic oxygen. The two original Pt peaks attributable to metallic Pt are also still present in the spectrum, but they are shifted 0.2 eV toward higher BEs. Comparing the percent concentrations of the Pt peaks before and after the treatment, we calculate that ~10% of the original Pt signal arises from oxygenated species after UV/O_3 treatment (Table 1 and 2).

For studies of electrocatalysis, we prefer to start with unoxidized Pt DENs, and therefore we attempted to reduce the oxygenated fraction of the Pt surface electrochemically. Specifically, after the UV/O_3 treatment, the PPF/G6-OH(Pt_{55}) electrode was scanned 10 times between −0.65 and 0.63 V in Ar-purged, 0.5 M H_2SO_4. As indicated by the XPS spectrum in Figure 2c, this electrochemical method was successful: the peaks arising from oxidize Pt (Figure 2b) are eliminated, and just the original two peaks, corresponding to metallic Pt, are present at 71.8 and 75.0 eV. Note, however, that these values are ~0.2 eV lower than those of the original Pt DENs (Figure 2a).

STEM can be used to image Pt DENs before and after UV/O_3 treatment to determine if there are gross morphological changes. Within the resolution of the microscope (point-to-point resolution of 0.19 nm), Figure 3 indicates no UV/O_3-induced changes. Specifically, the Pt DENs appear spherical and have an average diameter of ~1.4 ± 0.3 nm before and after treatment.

Location of Pt DENs. As discussed in the context of Figure 1, the UV/O_3 treatment presented here can be used to decompose most of the dendrimer templates from Pt DENs immobilized on PPF supports. To confirm removal of the dendrimers after the UV/O_3 treatment, however, we carried out a Pt surface poisoning experiment we have used previously to determine the location of the NPs.[26]

The poisoning experiment was performed on PPF/G6-OH(Pt_{55}) electrodes before and after UV/O_3 exposure using the following approach. First, a PPF/G6-OH(Pt_{55}) electrode that was not exposed to UV/O_3 was immersed in ethanol for 3 min, and then sufficient 1-decanethiol was added to the ethanol to make the solution 3.0 mM in the thiol. The electrode was left in this solution for 20 min. Second, the electrode was removed from the thiol solution and rinsed with ethanol and then with DI water. Finally, the potential of the electrode was scanned in an O_2-saturated, 0.5 M H_2SO_4 solution. The resulting cyclic voltammogram (CV), shown in red in Figure 4a, reveals a featureless shape characteristic of a passivated Pt surface. This result is interpreted as follows. Because ethanol is a good solvent for PAMAM dendrimers, the 1-decanethiol is able to diffuse through the dendrimer branches and adsorb to the Pt NP surface. This inhibits the inner-sphere oxygen reduction reactions (ORR).

Next, this same experiment was repeated, but now using CH_2Cl_2 instead of ethanol. CH_2Cl_2 is a poor solvent for PAMAM dendrimers, and in its presence the dendrimers collapse around the encapsulated NPs and protect them from being poisoned with 1-decanethiol. The resulting well-defined ORR peak (black CV in Figure 4a) obtained after this experiment confirms that the Pt DENs were encapsulated within the dendrimers during exposure to the thiol/CH_2Cl_2 solution.

The two experiments described previously were now carried out using PPF/G6-OH(Pt_{55}) electrodes following UV/O_3 exposure. The results of these experiments are summarized by Figure 4b. Now the CVs obtained after the poisoning experiments, using either ethanol (red CV) or CH_2Cl_2 (black CV), exhibit very low currents (note the difference in the

DOI: 10.1021/acs.langmuir.6b02578
Langmuir 2016, 32, 9727−9735

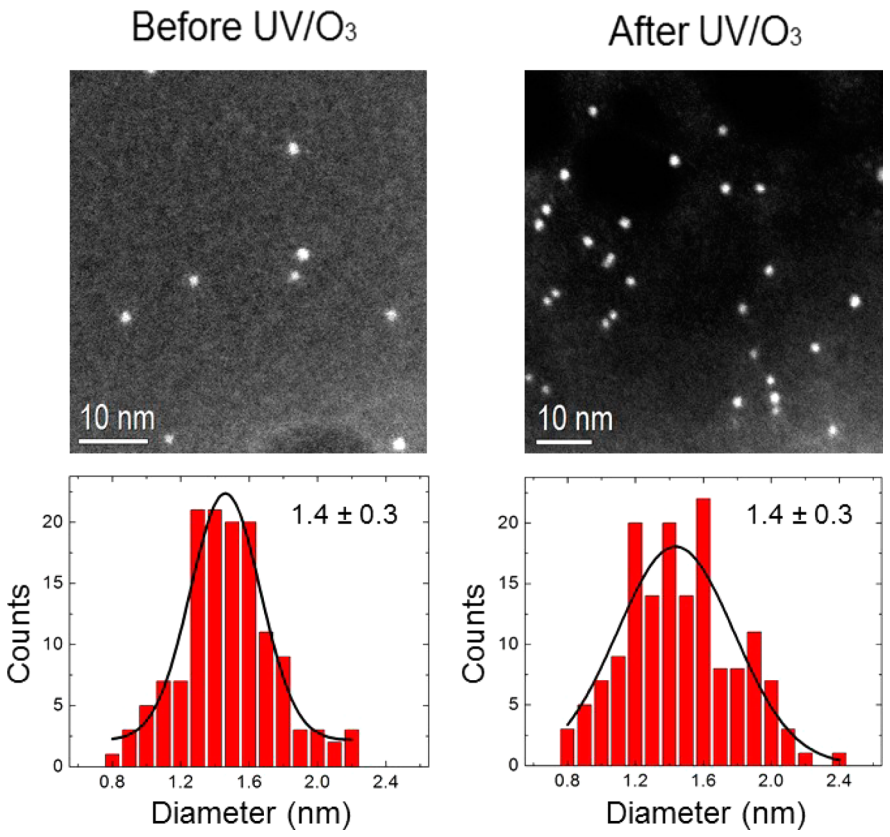

Figure 3. STEM micrographs and size-distribution histograms for G6-OH(Pt_{55}) DENs before (left) and after (right) UV/O_3 treatment. The size distribution is based on 200 randomly selected particles.

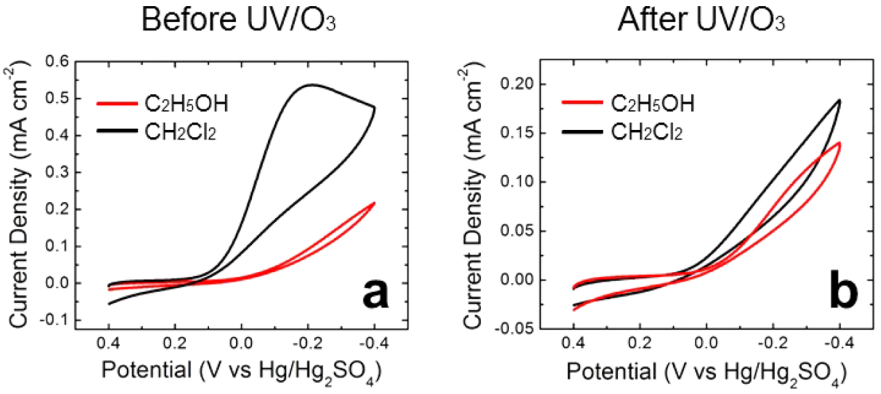

Figure 4. CVs obtained using PPF/G6-OH(Pt_{55}) electrodes (a) before and (b) after UV/O_3 treatment. In all cases the electrodes were exposed to 1-decanethiol in either CH_2Cl_2 (black) or ethanol (red) for 20 min. The aqueous 0.5 M H_2SO_4 solution was saturated with O_2. The scan rate was 50 mV/s.

current scales for Figures 4a,b). These observations are consistent with Pt NPs being present on the PPF support as naked NPs without dendrimers present to shield them from 1-decanethiol. We conclude that these electrochemical experiments confirm the XPS results: nearly all of the dendrimer is removed by the UV/O_3 treatment, and so the Pt surface is fully exposed to the solution.

The ORR in the Presence and Absence of Pt NP-PPF Support Interactions. The discussion up to this point demonstrates that UV/O_3 removes most of the dendrimer from the Pt DENs, and thus converts PPF/G6-OH(Pt_{55}) electrodes to PPF/Pt_{55} electrodes. Our ultimate objective in the series of studies that will follow this first report is to better understand how underlying supports affect electrocatalytic reactions. As a first step in that direction, we examined the ORR at PPF/G6-OH(Pt_{55}) and PPF/Pt_{55} electrodes.

Before obtaining CVs for the ORR, the Pt NPs were electrochemically cleaned in an Ar-saturated, 0.5 M H_2SO_4 solution. Immediately thereafter, the electrodes were immersed in an O_2-saturated 0.5 M H_2SO_4 solution, and then the potential was scanned between 0.40 V and −0.40 V (vs Hg/Hg_2SO_4). Figure 5 compares CVs obtained for the ORR before and after UV/O_3 exposure. The results indicate that both electrodes are electrochemically active for the ORR and yield similar CVs. On the basis of four independent experiments, however, there are slight differences. For example, the peak

DOI: 10.1021/acs.langmuir.6b02578
Langmuir 2016, 32, 9727−9735

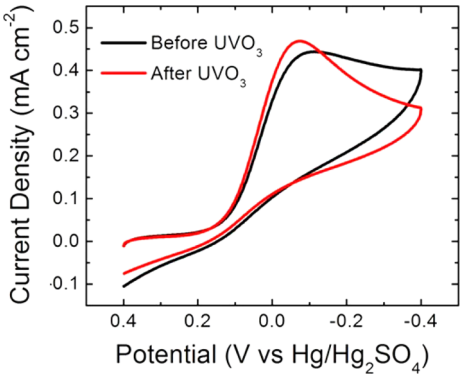

Figure 5. CVs obtained using PPF/G6-OH(Pt_{55}) electrodes and an aqueous 0.5 M H_2SO_4 solution saturated with O_2 before (black) and after (red) UV/O_3 treatment. The current density is based on the surface area of Pt determined by H-adsorption. The scan rate was 50 mV/s.

current potential shifts from −84 ± 6 mV before UV/O_3 treatment to −62 ± 6 mV after removal of the dendrimer, indicating a slight improvement in reaction kinetics. The value of the peak current density, however, does not change within the error of the measurement (0.44 ± 0.02 mA/cm^2 vs 0.49 ± 0.04 mA/cm^2 before and after UV/O_3 treatment, respectively). We cannot be sure of the reason for the slight favorable shift in the ORR peak position in the absence of the dendrimer, but it might be due to the appearance of a few additional catalytic sites on each Pt NP when the dendrimer is removed. As previously stated, however, the potential shift is very small and consistent with our previous claims that the presence of the dendrimer has little influence on the catalytic transformation of small molecules, like O_2, at the encapsulated DENs.[3,4] The results also indicate that the PPF electrode support has little effect on the ORR, which is also not surprising.

We also carried out chronoamperometric ORR experiments of the PPF/G6-OH(Pt_{55}) electrodes before and after UV/O_3 treatment (Supporting Information, Figure S-4). These data were obtained using an O_2-saturated, 0.5 M H_2SO_4 electrolyte solution and holding the electrode potential at −0.24 V (vs Hg/Hg_2SO_4) for 900 s. The results are consistent with the CVs shown in Figure 5: slightly faster turnover of O_2 after removal of the dendrimer.

SUMMARY AND CONCLUSIONS

Here we have shown that UV/O_3 can be used to almost entirely remove G6-OH PAMAM dendrimers from surface-confined Pt DENs without changing their size, shape, or electrocatalytic properties. These points are important for two reasons. First, they suggest that the dendrimer itself has very little influence on the electrocatalytic properties of the encapsulated NPs. This is important because it means that results obtained using DENs reliably extrapolate to the electrocatalytic properties of other types of naked NPs. Second, the fact that the dendrimer can be cleanly removed without significantly changing the DENs makes it possible to study electrocatalytic reactions in the presence and absence of support interactions (Scheme 1). In other words, this is a near-perfect system for studying support effects, because the exact same electrode can be examined with support effects turned on or off simply by removing the dendrimer by UV/O_3.

One last point. Fermin,[63−66] Gooding,[67,68] and others[69−76] have shown that electron transfer across thin insulating layers is not inhibited if NPs are present on the solution side of the insulator. We recently confirmed their findings using DENs as the NPs and ultrathin layers of Al_2O_3, deposited by atomic layer deposition, as the insulator.[25] Those findings, taken together with the results reported in this article, mean that it will now be possible for us to examine electrocatalytic reactions on essentially any oxide or nitride support using any type of catalytic DEN. These experiments are currently underway in our lab, and the results will be reported in due course.

ASSOCIATED CONTENT

Supporting Information

The Supporting Information is available free of charge on the ACS Publications website at DOI: 10.1021/acs.langmuir.6b02578.

High-resolution XPS O 1s spectra of a PPF/G6-OH(Pt_{55}) electrode before and after the UV/O_3 treatment; SEM micrographs of a PPF electrode before and after the UV/O_3 treatment; high-resolution XPS N 1s spectra of PPF modified with G6-OH at different pH values; chronoamperometry of the PPF/G6-OH(Pt_{55}) electrode before and after UV/O_3 treatment (PDF)

AUTHOR INFORMATION

Corresponding Author

*E-mail: crooks@cm.utexas.edu; Tel: 512-475-8674.

Notes

The authors declare no competing financial interest.

ACKNOWLEDGMENTS

We gratefully acknowledge support from the Chemical Sciences, Geosciences, and Biosciences Division, Office of Basic Energy Sciences, Office of Science, U.S. Department of Energy (Contract: DE-FG02-13ER16428). We thank the Robert A. Welch Foundation (Grant F-0032) for sustained support of our research. We also thank Dr. Hugo Celio (UT-Austin) for helpful discussions.

REFERENCES

(1) Bronstein, L. M.; Shifrina, Z. B. Dendrimers as Encapsulating, Stabilizing, or Directing Agents for Inorganic Nanoparticles. *Chem. Rev.* **2011**, *111*, 5301−5344.

(2) *Nanoparticles and Catalysis*; Astruc, D., Ed.; Wiley-VCH: Weinheim, Germany, 2008.

(3) Myers, V. S.; Weir, M. G.; Carino, E. V.; Yancey, D. F.; Pande, S.; Crooks, R. M. Dendrimer-Encapsulated Nanoparticles: New Synthetic and Characterization Methods and Catalytic Applications. *Chem. Sci.* **2011**, *2*, 1632.

(4) Anderson, R. M.; Yancey, D. F.; Zhang, L.; Chill, S. T.; Henkelman, G.; Crooks, R. M. A Theoretical and Experimental Approach for Correlating Nanoparticle Structure and Electrocatalytic Activity. *Acc. Chem. Res.* **2015**, *48*, 1351−1357.

(5) Anderson, R. M.; Zhang, L.; Wu, D.; Brankovic, S. R.; Henkelman, G.; Crooks, R. M. A Theoretical and Experimental In-Situ Electrochemical Infrared Spectroscopy Study of Adsorbed CO on Pt Dendrimer-Encapsulated Nanoparticles. *J. Electrochem. Soc.* **2016**, *163*, H3061−H3065.

(6) Lang, H.; May, R. A.; Iversen, B. L.; Chandler, B. D. Dendrimer-Encapsulated Nanoparticle Precursors to Supported Platinum Catalysts. *J. Am. Chem. Soc.* **2003**, *125*, 14832−14836.

(7) Crump, C. J.; Gilbertson, J. D.; Chandler, B. D. CO Oxidation and Toluene Hydrogenation by Pt/TiO_2 Catalysts Prepared from Dendrimer Encapsulated Nanoparticle Precursors. *Top. Catal.* **2008**, *49*, 233−240.

DOI: 10.1021/acs.langmuir.6b02578
Langmuir 2016, 32, 9727−9735

(8) Peng, X.; Pan, Q.; Rempel, G. L. Bimetallic Dendrimer-Encapsulated Nanoparticles as Catalysts: A Review of the Research Advances. *Chem. Soc. Rev.* **2008**, *37*, 1619.
(9) Zhang, L.; Anderson, R. M.; Crooks, R. M.; Henkelman, G. Correlating Structure and Function of Metal Nanoparticles for Catalysis. *Surf. Sci.* **2015**, *640*, 65−72.
(10) Niu, Y.; Crooks, R. M. Dendrimer-Encapsulated Metal Nanoparticles and Their Applications to Catalysis. *C. R. Chim.* **2003**, *6*, 1049−1059.
(11) Buhleier, E.; Wehner, W.; Vogtle, F. 'Cascade' - and 'Nonskid-Chain-Like' Synthesis of Molecular Cavity Topologies. *Chem. Informationsdienst* **1978**, DOI: 10.1002/chin.197825228.
(12) Scott, R. W. J.; Wilson, O. M.; Crooks, R. M. Synthesis, Characterization, and Applications of Dendrimer-Encapsulated Nanoparticles. *J. Phys. Chem. B* **2005**, *109*, 692−704.
(13) Patel, H. N.; Patel, P. M. Dendrimer Applications−a Review. *Int. J. Pharm. Bio Sci.* **2013**, *4*, 454−463.
(14) Singh, I.; Rehni, A. K.; Kalra, R.; Joshi, G.; Kumar, M. Dendrimers and Their Pharmaceutical Applications−a Review. *Pharm.- Int. J. Pharm. Sci.* **2008**, *63*, 491−496.
(15) Menjoge, A. R.; Kannan, R. M.; Tomalia, D. A. Dendrimer-Based Drug and Imaging Conjugates: Design Considerations for Nanomedical Applications. *Drug Discovery Today* **2010**, *15*, 171−185.
(16) Tsai, E. Dendrimer-Encapsulated Nanoparticles: Vehicles for Drug Delivery, with an Emphasis on PAMAM Dendrimers. *COSMOS* **2011**, *8*, 1−16.
(17) Shadrack, D.; Mubofu, E.; Nyandoro, S. Synthesis of Polyamidoamine Dendrimer for Encapsulating Tetramethylscutellarein for Potential Bioactivity Enhancement. *Int. J. Mol. Sci.* **2015**, *16*, 26363−26377.
(18) Dendritech, PAMAM Dendrimers. Http://www.dendritech.com/pamam.html (Accessed Apr 16, 2016).
(19) Anderson, R. M.; Yancey, D. F.; Loussaert, J. A.; Crooks, R. M. Multistep Galvanic Exchange Synthesis Yielding Fully Reduced Pt Dendrimer-Encapsulated Nanoparticles. *Langmuir* **2014**, *30*, 15009−15015.
(20) Zheng, J.; Zhang, C.; Dickson, R. M. Highly Fluorescent, Water-Soluble, Size-Tunable Gold Quantum Dots. *Phys. Rev. Lett.* **2004**, *93*, 077402.
(21) Petty, J. T.; Fan, C.; Story, S. P.; Sengupta, B.; St. John Iyer, A.; Prudowsky, Z.; Dickson, R. M. DNA Encapsulation of 10 Silver Atoms Producing a Bright, Modulatable, Near-Infrared-Emitting Cluster. *J. Phys. Chem. Lett.* **2010**, *1*, 2524−2529.
(22) Oh, S.-K.; Kim, Y.-G.; Ye, H.; Crooks, R. M. Synthesis, Characterization, and Surface Immobilization of Metal Nanoparticles Encapsulated within Bifunctionalized Dendrimers. *Langmuir* **2003**, *19*, 10420−10425.
(23) Yeung, L. K.; Lee, C. T., Jr; Johnston, K. P.; Crooks, R. M. Catalysis in Supercritical CO2 Using Dendrimer-Encapsulated Palladium Nanoparticles. *Chem. Commun.* **2001**, 2290−2291.
(24) Garcia-Martinez, J. C.; Crooks, R. M. Extraction of Au Nanoparticles Having Narrow Size Distributions from within Dendrimer Templates. *J. Am. Chem. Soc.* **2004**, *126*, 16170−16178.
(25) Ostojic, N.; Thorpe, J. H.; Crooks, R. M. Electron Transfer Facilitated by Dendrimer-Encapsulated Pt Nanoparticles Across Ultrathin, Insulating Oxide Films. *J. Am. Chem. Soc.* **2016**, *138*, 6829−6837.
(26) Ye, H.; Crooks, R. M. Electrocatalytic O_2 Reduction at Glassy Carbon Electrodes Modified with Dendrimer-Encapsulated Pt Nanoparticles. *J. Am. Chem. Soc.* **2005**, *127*, 4930−4934.
(27) Albiter, M. A.; Crooks, R. M.; Zaera, F. Adsorption of Carbon Monoxide on Dendrimer-Encapsulated Platinum Nanoparticles: Liquid versus Gas Phase. *J. Phys. Chem. Lett.* **2010**, *1*, 38−40.
(28) Schalley, C. A.; Verhaelen, C.; Klärner, F.-G.; Hahn, U.; Vögtle, F. Gas-Phase Host-Guest Chemistry of Dendritic Viologens and Molecular Tweezers: A Remarkably Strong Effect on Dication Stability. *Angew. Chem., Int. Ed.* **2005**, *44*, 477−480.
(29) Schalley, C. A.; Baytekin, B.; Baytekin, H. T.; Engeser, M.; Felder, T.; Rang, A. Mass Spectrometry as a Tool in Dendrimer Chemistry: From Self-Assembling Dendrimers to Dendrimer Gas-Phase Host−guest Chemistry. *J. Phys. Org. Chem.* **2006**, *19*, 479−490.
(30) Schalley, C. A. Molecular Recognition and Supramolecular Chemistry in the Gas Phase. *Mass Spectrom. Rev.* **2001**, *20*, 253−309.
(31) Luo, L.; Zhang, L.; Henkelman, G.; Crooks, R. M. Unusual Activity Trend for CO Oxidation on Pd_X Au_{140-X} @Pt Core@Shell Nanoparticle Electrocatalysts. *J. Phys. Chem. Lett.* **2015**, *6*, 2562−2568.
(32) Fu, Q.; Yang, F.; Bao, X. Interface-Confined Oxide Nanostructures for Catalytic Oxidation Reactions. *Acc. Chem. Res.* **2013**, *46*, 1692−1701.
(33) Freund, H.-J.; Heyde, M.; Nilius, N.; Schauermann, S.; Shaikhutdinov, S.; Sterrer, M. Model Studies on Heterogeneous Catalysts at the Atomic Scale: From Supported Metal Particles to Two-Dimensional Zeolites. *J. Catal.* **2013**, *308*, 154−167.
(34) Pacchioni, G. Electronic Interactions and Charge Transfers of Metal Atoms and Clusters on Oxide Surfaces. *Phys. Chem. Chem. Phys.* **2013**, *15*, 1737.
(35) Geukens, I.; De Vos, D. E. Organic Transformations on Metal Nanoparticles: Controlling Activity, Stability, and Recyclability by Support and Solvent Interactions. *Langmuir* **2013**, *29*, 3170−3178.
(36) Liu, J. J. Advanced Electron Microscopy of Metal-Support Interactions in Supported Metal Catalysts. *ChemCatChem* **2011**, *3*, 934−948.
(37) Calle-Vallejo, F.; Koper, M. T. M.; Bandarenka, A. S. Tailoring the Catalytic Activity of Electrodes with Monolayer Amounts of Foreign Metals. *Chem. Soc. Rev.* **2013**, *42*, 5210.
(38) Aliaga, C.; Park, J. Y.; Yamada, Y.; Lee, H. S.; Tsung, C.-K.; Yang, P.; Somorjai, G. A. Sum Frequency Generation and Catalytic Reaction Studies of the Removal of Organic Capping Agents from Pt Nanoparticles by UV−Ozone Treatment. *J. Phys. Chem. C* **2009**, *113*, 6150−6155.
(39) Ozturk, O.; Black, T. J.; Perrine, K.; Pizzolato, K.; Williams, C. T.; Parsons, F. W.; Ratliff, J. S.; Gao, J.; Murphy, C. J.; Xie, H.; et al. Thermal Decomposition of Generation-4 Polyamidoamine Dendrimer Films: Decomposition Catalyzed by Dendrimer-Encapsulated Pt Particles. *Langmuir* **2005**, *21*, 3998−4006.
(40) Deutsch, D. S.; Lafaye, G.; Liu, D.; Chandler, B.; Williams, C. T.; Amiridis, M. D. Decomposition and Activation of Pt-Dendrimer Nanocomposites on a Silica Support. *Catal. Lett.* **2004**, *97*, 139−143.
(41) Santiago-Morales, J.; Rosal, R.; Hernando, M. D.; Ulaszewska, M. M.; García-Calvo, E.; Fernández-Alba, A. R. Fate and Transformation Products of Amine-Terminated PAMAM Dendrimers under Ozonation and Irradiation. *J. Hazard. Mater.* **2014**, *266*, 102−113.
(42) Borodko, Y.; Thompson, C. M.; Huang, W.; Yildiz, H. B.; Frei, H.; Somorjai, G. A. Spectroscopic Study of Platinum and Rhodium Dendrimer (PAMAM G4OH) Compounds: Structure and Stability. *J. Phys. Chem. C* **2011**, *115*, 4757−4767.
(43) Lewera, A.; Timperman, L.; Roguska, A.; Alonso-Vante, N. Metal−Support Interactions between Nanosized Pt and Metal Oxides (WO_3 and TiO_2) Studied Using X-Ray Photoelectron Spectroscopy. *J. Phys. Chem. C* **2011**, *115*, 20153−20159.
(44) Sasaki, K.; Zhang, L.; Adzic, R. R. Niobium Oxide-Supported Platinum Ultra-Low Amount Electrocatalysts for Oxygen Reduction. *Phys. Chem. Chem. Phys.* **2008**, *10*, 159−167.
(45) Baturina, O. A.; Garsany, Y.; Zega, T. J.; Stroud, R. M.; Schull, T.; Swider-Lyons, K. E. Oxygen Reduction Reaction on Platinum/Tantalum Oxide Electrocatalysts for PEM Fuel Cells. *J. Electrochem. Soc.* **2008**, *155*, B1314.
(46) Garsany, Y.; Epshteyn, A.; Purdy, A. P.; More, K. L.; Swider-Lyons, K. E. High-Activity, Durable Oxygen Reduction Electrocatalyst: Nanoscale Composite of Platinum−Tantalum Oxyphosphate on Vulcan Carbon. *J. Phys. Chem. Lett.* **2010**, *1*, 1977−1981.
(47) Korovina, A.; Garsany, Y.; Epshteyn, A.; Purdy, A. P.; More, K.; Swider-Lyons, K. E.; Ramaker, D. E. Understanding Oxygen Reduction on Tantalum Oxyphosphate and Tantalum Oxide Supported Platinum by X-Ray Absorption Spectroscopy. *J. Phys. Chem. C* **2012**, *116*, 18175−18183.
(48) Zhou, W.-P.; Axnanda, S.; White, M. G.; Adzic, R. R.; Hrbek, J. Enhancement in Ethanol Electrooxidation by SnO_X Nanoislands

DOI: 10.1021/acs.langmuir.6b02578
Langmuir 2016, 32, 9727−9735

Grown on Pt(111): Effect of Metal Oxide−Metal Interface Sites. *J. Phys. Chem. C* **2011**, *115*, 16467−16473.
(49) Zhou, W.-P.; An, W.; Su, D.; Palomino, R.; Liu, P.; White, M. G.; Adzic, R. R. Electrooxidation of Methanol at SnO_X − Pt Interface: A Tunable Activity of Tin Oxide Nanoparticles. *J. Phys. Chem. Lett.* **2012**, *3*, 3286−3290.
(50) Sasaki, K.; Adzic, R. R. Monolayer-Level Ru- and NbO[sub 2]-Supported Platinum Electrocatalysts for Methanol Oxidation. *J. Electrochem. Soc.* **2008**, *155*, B180.
(51) Li, M.; Cullen, D. A.; Sasaki, K.; Marinkovic, N. S.; More, K.; Adzic, R. R. Ternary Electrocatalysts for Oxidizing Ethanol to Carbon Dioxide: Making Ir Capable of Splitting C−C Bond. *J. Am. Chem. Soc.* **2013**, *135*, 132−141.
(52) Li, M.; Zhou, W.-P.; Marinkovic, N. S.; Sasaki, K.; Adzic, R. R. The Role of Rhodium and Tin Oxide in the Platinum-Based Electrocatalysts for Ethanol Oxidation to CO_2. *Electrochim. Acta* **2013**, *104*, 454−461.
(53) Ranganathan, S.; Mccreery, R.; Majji, S. M.; Madou, M. Photoresist-Derived Carbon for Microelectromechanical Systems and Electrochemical Applications. *J. Electrochem. Soc.* **2000**, *147*, 277−282.
(54) Ranganathan, S.; McCreery, R. L. Electroanalytical Performance of Carbon Films with Near-Atomic Flatness. *Anal. Chem.* **2001**, *73*, 893−900.
(55) Kostecki, R.; Schnyder, B.; Alliata, D.; Song, X.; Kinoshita, K.; Kotz, R. Surface Studies of Carbon Films from Pyrolyzed Photoresist. *Thin Solid Films* **2001**, *396*, 36−43.
(56) Kim, J.; Song, X.; Kinoshita, K.; Madou, M.; White, R. Electrochemical Studies of Carbon Films from Pyrolyzed Photoresist. *J. Electrochem. Soc.* **1998**, *145*, 2314.
(57) Pande, S.; Weir, M. G.; Zaccheo, B. A.; Crooks, R. M. Synthesis, Characterization, and Electrocatalysis Using Pt and Pd Dendrimer-Encapsulated Nanoparticles Prepared by Galvanic Exchange. *New J. Chem.* **2011**, *35*, 2054.
(58) *NIST X-Ray Photoelectron Spectroscopy Database*, Version 4.1;National Institute of Standards and Technology: Gaithersburg, MD, 2012 (http://srdata.nist.gov/xps/).
(59) Ultraviolet-Ozone Surface Treatment. *ThreeBond Technical News* 1987, 1−10.
(60) Vig, J. R. UV/ozone Cleaning of Surfaces. *J. Vac. Sci. Technol., A* **1985**, *3*, 1027.
(61) Loussaert, J. A.; Fosdick, S. E.; Crooks, R. M. Electrochemical Properties of Metal-Oxide-Coated Carbon Electrodes Prepared by Atomic Layer Deposition. *Langmuir* **2014**, *30*, 13707−13715.
(62) Tokuhisa, H.; Zhao, M.; Baker, L. A.; Phan, V. T.; Dermody, D. L.; Garcia, M. E.; Peez, R. F.; Crooks, R. M.; Mayer, T. M. Preparation and Characterization of Dendrimer Monolayers and Dendrimer-Alkanethiol Mixed Monolayers Adsorbed to Gold. *J. Am. Chem. Soc.* **1998**, *120*, 4492−4501.
(63) Zhao, J.; Bradbury, C. R.; Fermin, D. J. Long-Range Electronic Communication between Metal Nanoparticles and Electrode Surfaces Separated by Polyelectrolyte Multilayer Films. *J. Phys. Chem. C* **2008**, *112*, 6832−6841.
(64) Kissling, G. P.; Miles, D. O.; Fermín, D. J. Electrochemical Charge Transfer Mediated by Metal Nanoparticles and Quantum Dots. *Phys. Chem. Chem. Phys.* **2011**, *13*, 21175.
(65) Zhao, J.; Bradbury, C. R.; Huclova, S.; Potapova, I.; Carrara, M.; Fermín, D. J. Nanoparticle-Mediated Electron Transfer Across Ultrathin Self-Assembled Films. *J. Phys. Chem. B* **2005**, *109*, 22985−22994.
(66) Bradbury, C. R.; Zhao, J.; Fermín, D. J. Distance-Independent Charge-Transfer Resistance at Gold Electrodes Modified by Thiol Monolayers and Metal Nanoparticles. *J. Phys. Chem. C* **2008**, *112*, 10153−10160.
(67) Shein, J. B.; Lai, L. M. H.; Eggers, P. K.; Paddon-Row, M. N.; Gooding, J. J. Formation of Efficient Electron Transfer Pathways by Adsorbing Gold Nanoparticles to Self-Assembled Monolayer Modified Electrodes. *Langmuir* **2009**, *25*, 11121−11128.
(68) Barfidokht, A.; Ciampi, S.; Luais, E.; Darwish, N.; Gooding, J. J. Distance-Dependent Electron Transfer at Passivated Electrodes Decorated by Gold Nanoparticles. *Anal. Chem.* **2013**, *85*, 1073−1080.
(69) Grabar, K. C.; Allison, K. J.; Baker, B. E.; Bright, R. M.; Brown, K. R.; Freeman, R. G.; Fox, A. P.; Keating, C. D.; Musick, M. D.; Natan, M. J. Two-Dimensional Arrays of Colloidal Gold Particles: A Flexible Approach to Microscopic Metal Surfaces. *Langmuir* **1996**, *12*, 2353−2361.
(70) Freeman, R. G.; Grabar, K. C.; Allison, K. J.; Bright, R. M.; Davis, J. A.; Guthrie, A. P.; Hommer, M. B.; Jackson, M. A.; Smith, P. C.; Walter, D. G.; et al. Self-Assembled Metal Colloids Monolayers: An Approach to SERS Substrates. *Science* **1995**, *267*, 1629.
(71) Bethell, D.; Brust, M.; Schiffrin, D. J.; Kiely, C. From Monolayers to Nanostructured Materials: An Organic Chemist's View of Self-Assembly. *J. Electroanal. Chem.* **1996**, *409*, 137−143.
(72) Brust, M.; Bethell, D.; Kiely, C. J.; Schiffrin, D. J. Self-Assembled Gold Nanoparticle Thin Films with Nonmetallic Optical and Electronic Properties. *Langmuir* **1998**, *14*, 5425−5429.
(73) Horswell, S. L.; O'Nei, I. A.; Schiffrin, D. J. Kinetics of Electron Transfer at Pt Nanostructured Film Electrodes. *J. Phys. Chem. B* **2003**, *107*, 4844−4854.
(74) Nuzzo, R. G.; Allara, D. L. Adsorption of Bifunctional Organic Disulfides on Gold Surfaces. *J. Am. Chem. Soc.* **1983**, *105*, 4481−4483.
(75) Hill, C. M.; Kim, J.; Bard, A. J. Electrochemistry at a Metal Nanoparticle on a Tunneling Film: A Steady-State Model of Current Densities at a Tunneling Ultramicroelectrode. *J. Am. Chem. Soc.* **2015**, *137*, 11321−11326.
(76) Kim, H. J.; Kearney, K. L.; Le, L. H.; Pekarek, R. T.; Rose, M. J. Platinum-Enhanced Electron Transfer and Surface Passivation through Ultrathin Film Aluminum Oxide (Al_2O_3) on Si(111)−CH_3 Photoelectrodes. *ACS Appl. Mater. Interfaces* **2015**, *7*, 8572−8584.

DOI: 10.1021/acs.langmuir.6b02578
Langmuir 2016, 32, 9727−9735